



Study of the solid-phase equilibria in the GeTe-Bi₂Te₃-Te system and thermodynamic properties of GeTe-rich germanium bismuth tellurides

E.N. Orujlu^{a,*}, D.M. Babanly^{b,c}, T.M. Alakbarova^d, N.I. Orujov^e, M.B. Babanly^{c,d,f,*}

^a Azerbaijan State Oil and Industry University, AZ1010 Baku, Azerbaijan

^b French-Azerbaijani University (UFAZ), AZ1010 Baku, Azerbaijan

^c Institute of Catalysis and Inorganic Chemistry, AZ1143 Baku, Azerbaijan

^d Baku State University, AZ1148 Baku, Azerbaijan

^e Baku Engineering University, AZ0101 Khirdalan, Azerbaijan

^f Azerbaijan State University of Economics. AZ1001 Baku, Azerbaijan

ARTICLE INFO

Keywords:

Germanium-bismuth tellurides
Electromotive force
EMF
Thermodynamic properties
Solid-phase equilibria

ABSTRACT

A set of self-consistent thermodynamic parameters of the GeTe-rich germanium-bismuth tellurides were determined using an electromotive force (EMF) method with a glycerol electrolyte in a temperature range from 300 to 450 K. The solid-phase equilibrium diagram of the GeTe-Bi₂Te₃-Te system at 400 K was constructed using X-ray diffraction (XRD) and scanning electron microscope (SEM) techniques of synthesized electrode alloys, as well as available literature data. It is found that all telluride phases in GeTe-Bi₂Te₃ pseudo-binary section have a tie-line connection with elemental tellurium. The relative partial thermodynamic functions of GeTe in alloys were calculated using data from EMF measurements of concentration cells relative to the GeTe electrode. These findings together with the corresponding thermodynamic functions of GeTe and Bi₂Te₃ were used to calculate the relative partial molar functions of germanium in alloys, and also the standard thermodynamic functions of formation and standard entropies of the ternary compounds, namely Ge₂Bi₂Te₅, Ge₃Bi₂Te₆ and Ge₄Bi₂Te₇.

1. Introduction

Germanium-based chalcogenide materials have been shown to exhibit a good combination of thermoelectric, electronic, optical, topological insulator (TI), etc. properties that makes them suitable for the development of new generation technologies, such as mid-temperature power generation [1,2], optical displays [3,4], photonic memory [5,6], neuro-inspired computing [7–9], and so on. Among these chalcogenide phases, ternary tetradymite-type layered compounds of the GeTe-Sb(Bi)₂Te₃ pseudo-binary tie-line have witnessed special interest for their phase-change properties and a novel electronic state – TI properties that have emerged in recent years. The ability of amorphous–crystalline phase transitions by applying voltage or laser pulses is exploited for memory devices and germanium antimony (bismuth) tellurides have been extensively examined and considered one of the most successful materials for such applications [10–15]. On the other hand, both theoretical and experimental studies provided direct evidence for the existence of topological surface states in these materials as well

[16–21]. In this connection, detailed information on the phase equilibrium studies and accurate thermodynamic data of the corresponding ternary systems is crucially needed for understanding the nature of the chemical interaction and technological applications of these materials [22].

The present study is part of an ongoing research project that is aimed at developing accurate thermodynamic data for germanium bismuth tellurides which is essential for alloy design, synthesizing novel complex phases, and the development of their modern sample-preparation techniques.

Several versions of the phase diagram of the GeTe-Bi₂Te₃ pseudo-binary system exist in the literature, which all differ particularly in the number and melting behavior of the ternary compounds [23–27]. The latest constructed phase diagram which is given by us in [28] reports a total of six ternary compounds, including Ge₄Bi₂Te₇, Ge₃Bi₂Te₆, Ge₂Bi₂Te₅, GeBi₂Te₄, GeBi₄Te₇, and GeBi₆Te₁₀ in the system. It is found that Ge₄Bi₂Te₇ and Ge₃Bi₂Te₆ decompose by solid phase reactions, while the other four compounds are formed by peritectic reactions. Besides, it

* Corresponding authors at: Azerbaijan State Oil and Industry University, AZ1010 Baku, Azerbaijan (E.N. Orujlu); Institute of Catalysis and Inorganic Chemistry, AZ1143 Baku, Azerbaijan (M.B. Babanly).

E-mail addresses: elnur.oruclu@yahoo.com (E.N. Orujlu), babanlymb@gmail.com (M.B. Babanly).

<https://doi.org/10.1016/j.jct.2024.107323>

Received 12 October 2023; Received in revised form 23 April 2024; Accepted 4 May 2024

Available online 6 May 2024

0021-9614/© 2024 Elsevier Ltd.

Table 1
Provenance and purity of the materials used in this investigation.

Chemical	Mass fraction of purity	Source	CAS No	Form	Purity analysis methods
Ge	0.99999	Alfa Aesar (Germany)	7440–56-4	pieces	As stated by the supplier
Bi	0.99999	Alfa Aesar (Germany)	7440–69-9	shot	As stated by the supplier
Te	0.99999	Alfa Aesar (Germany)	13494–80-9	lump	As stated by the supplier
GeTe	0.999	synthesized by us	12025–39-7	ingot	DTA, XRD
Bi ₂ Te ₃	0.999	synthesized by us	1304–82-1	ingot	DTA, XRD

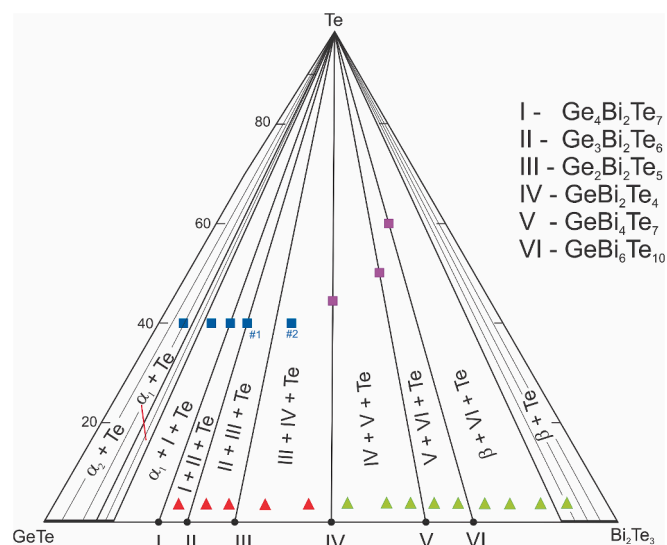


Fig. 1. Solid-phase equilibrium diagram of the GeTe-Bi₂Te₃-Te system at 400 K. Triangles (red) represents studied alloys for EMF measurements, while squares (blue) for XRD. Purple and green symbols represent studied compositions in our previous work in [29]. (For interpretation of the references to colour in this figure legend, the reader is referred to the web version of this article.)

is noted that the GeTe-based solubility in the system is ~ 13 mol%, and a mixture of GeTe-based cubic and layered phases is found in the samples as the composition shifts toward Bi₂Te₃. Since the intensity of the diffraction lines belonging to layered phases is very low in the more GeTe-rich samples, it is not possible to give an opinion on which phase they belong and these results greatly increase the possibility of new mixed layered compounds in the system.

In our previous work [29], we constructed a solid-phase equilibrium diagram of the GeBi₂Te₄-Bi₂Te₃-Te fragment in the GeTe-Bi₂Te₃-Te system and calculate a standard Gibbs free energy and enthalpy of formation, as well as the standard entropy of the GeBi₂Te₄, GeBi₄Te₇, GeBi₆Te₁₀ ternary compounds. Here, we report the most recent and accurate description of the solid-phase equilibrium diagram of the GeTe-Bi₂Te₃-Te system and thermodynamic properties of GeTe-rich germanium-antimony tellurides under standard conditions.

2. Experimental details

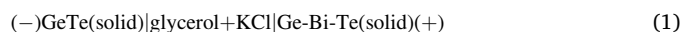
In the first stage, GeTe and Bi₂Te₃ binary compounds were synthesized. The purity of used elements was 99.999 wt% (see Table 1). Pre-determined amounts of elements were weighed with an analytical balance, then mixtures were put into quartz tubes and sealed under a vacuum. After synthesis, their phase purity was examined using powder X-ray diffraction (XRD) and differential thermal analysis (DTA) methods.

Alloys were prepared by melting accurately weighted amounts of pure initially synthesized starting binary compounds GeTe, Bi₂Te₃, and elemental tellurium. The design compositions of the alloys are given in Fig. 1 with square (blue) and triangle (red) symbols. Each alloy mixture was heated to 950 K and kept at this temperature for 5 h, and completed with rapid water quenching. Then the quenched samples were annealed stepwise at 700 K (1000 h) and 400 K (100 h) to ensure the establishment of an equilibrium state. The content of each sample was checked by powder XRD and scanning electron microscope (SEM) analysis.

The DTA investigations were carried out using LINSEIS HDSC PT1600 system at the rate of 10 K/min. Powder XRD was carried out using Cu-K α_1 radiation on Bruker D2 PHASER diffractometer. The microstructures and composition of phases in the samples were examined by Tescan Vega 3 SBH Scanning Electron Microscope. Electromotive force (EMF) measurements were performed using a Keithley 2100 6 1/2 Digit Multimeter (10^{14} Ω input resistance).

Measuring the EMF of electrochemical cells in order to calculate integral thermodynamic quantities is a very well-known and successfully used method for metal chalcogenides systems [29–36].

To study the thermodynamic properties of phases, the electrochemical cell type (1) was assembled for EMF measurements in the 300–450 K temperature interval. The cell arrangement was:



In the measurements, polyvalent alcohol – the glycerol solution of KCl was used as an electrolyte. Up to now, glycerol is successfully used for the low-temperature thermodynamic analysis of chalcogenide systems in numerous works [29,35,36]. Just like in our previous EMF study in [29], Ge²⁺ ion-containing salt was not added to the electrolyte at this time as well since its equilibrium concentration is very low and can be provided by the electrochemical cell itself. To prevent oxygen and moisture having into the electrolyte, the glycerol was properly dried and degassed under vacuum at 450 K before being filled into the electrochemical cell. Anhydrous chemically pure KCl salt was used.

For EMF measurements, GeTe was chosen as a negative electrode, while the positive electrode was made of annealed alloys of the GeTe-Bi₂Te₃-Te system. Their compositions are shown in Fig. 1 with triangles. To prepare electrodes, GeTe, and synthesized alloys were powdered in an agate mortar, then pressed into molybdenum wire which forms pellets each weighing 0.5 g and a diameter of 7 mm.

More detailed information about preparation electrodes and assembling an electrochemical cell is described in [37–39]. A constructed electrochemical cell in this form allows for measuring the EMF values of several electrodes relative to one reference electrode at the same time.

After maintaining the electrochemical cell at 350 K for 40–60 h, the first EMF equilibrium values were recorded. The next values were obtained every 3–4 h after reaching the desired temperature. The system was considered to achieve an equilibrium state when the scatter was less than 0.5 mV. The reversibility of the constructed concentration cells was controlled by the fact that masses and phase compositions of electrodes were maintained constant during measurements.

3. Results and discussion

In order to study the thermodynamic properties of GeTe-rich germanium bismuth tellurides, a solid-phase equilibrium diagram of the GeTe-Bi₂Te₃-Te system was constructed at the first stage. In our previous work in [29], we showed that all telluride phases are in a tie-line connection with elementary tellurium in the GeBi₂Te₄-Bi₂Te₃-Te concentration range. In order to determine phase equilibria in the GeTe-Bi₂Te₃-Te system, several compositions were chosen to synthesize taking into account of the phase diagram of the GeTe-Bi₂Te₃ system. The results of the GeTe-rich region show that other ternary compounds and telluride phases have a tie-line connection with tellurium as well and the solid-phase equilibrium diagram of the GeTe-Bi₂Te₃-Te system has a similar

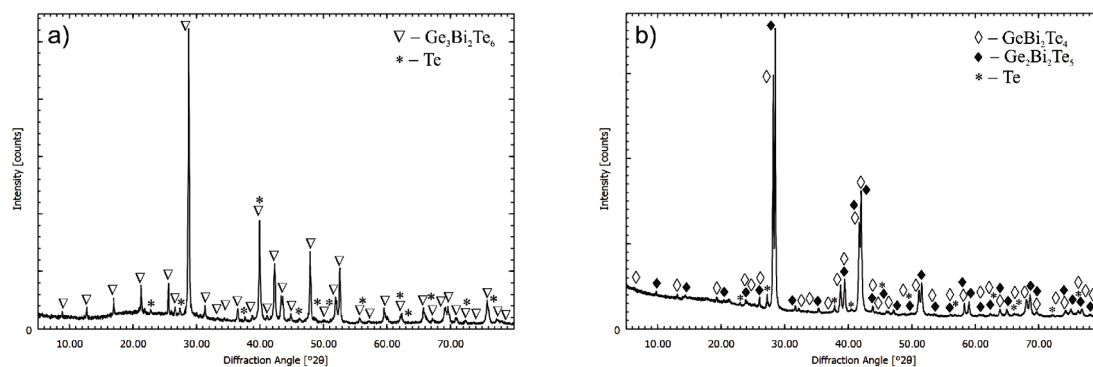


Fig. 2. XRD results of sample #1 and #2 in Figure 1.

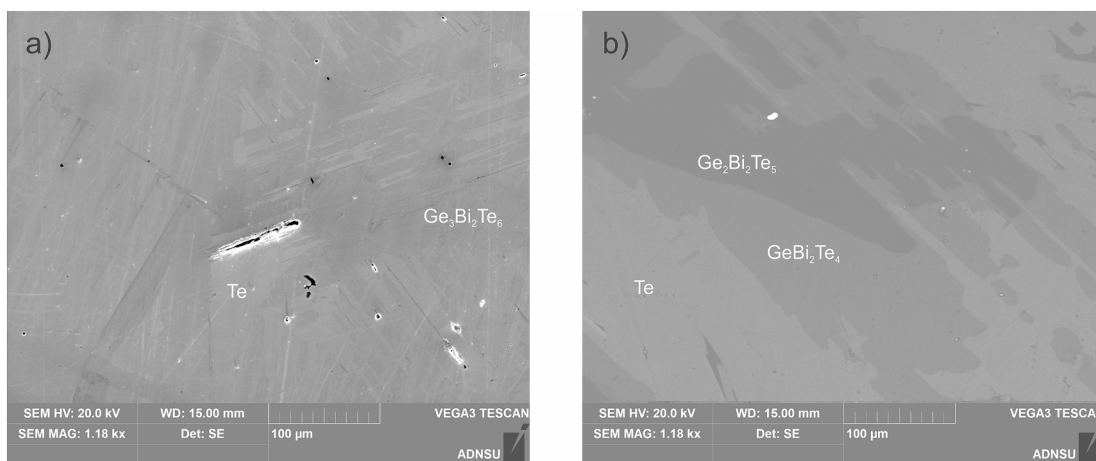


Fig. 3. The SEM images of sample #1 (a) and #2 (b).

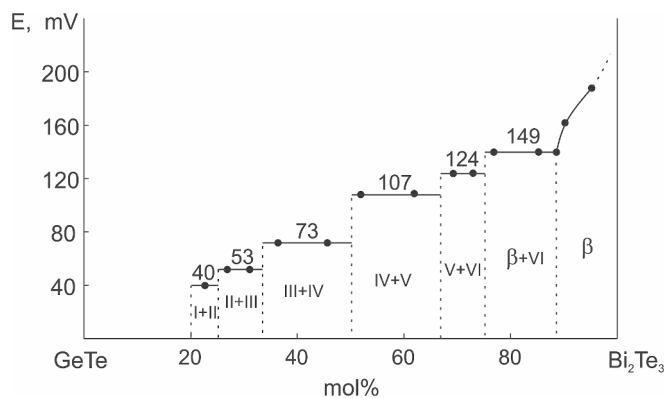


Fig. 4. The composition dependences of the EMF of type (1) cells at 400 K (see Supplementary data – Table S1–3). Here I – $\text{Ge}_4\text{Bi}_2\text{Te}_7$, II – $\text{Ge}_3\text{Bi}_2\text{Te}_6$, III – $\text{Ge}_2\text{Bi}_2\text{Te}_5$, IV – GeBi_2Te_4 , V – GeBi_4Te_7 , VI – $\text{GeBi}_6\text{Te}_{10}$, β – solid solution based on Bi_2Te_3 .

view as given in Fig. 1. This leads to the formation of a variety of heterogeneous zones in the system, and XRD results of different alloys taken from those areas confirm their phase compositions. As an example, Fig. 2 shows XRD patterns of representative alloys named sample #1 and #2. XRD identification, as shown in Fig. 2a confirmed the existence of the two phases of $\text{Ge}_3\text{Bi}_2\text{Te}_6$ and tellurium since this alloy composition is located on the tie-line. Sample #2 clearly demonstrated that $\text{Ge}_2\text{Bi}_2\text{Te}_5$ and GeBi_2Te_4 phases were in equilibrium with Te which is shown in Fig. 2b. The corresponding compositions of the equilibrium phases in the

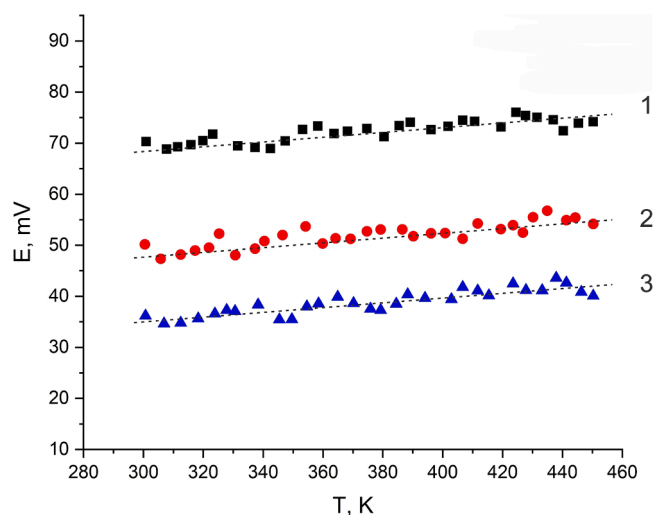


Fig. 5. The temperature dependences of EMF of the concentration cells type (1) for different phase regions of the GeTe- Bi_2Te_3 -Te system in Fig. 1: 1 – $\text{GeBi}_2\text{Te}_4 + \text{Ge}_2\text{Bi}_2\text{Te}_5 + \text{Te}$; 2 – $\text{Ge}_2\text{Bi}_2\text{Te}_5 + \text{Ge}_3\text{Bi}_2\text{Te}_6 + \text{Te}$; 3 – $\text{Ge}_3\text{Bi}_2\text{Te}_6 + \text{Ge}_4\text{Bi}_2\text{Te}_7 + \text{Te}$. Standard uncertainties are $u_E = 0.8$ mV, $u_T = 0.85$ K.

samples were further verified using SEM as well. The existence of two and three-phase equilibrium microstructures is clearly visible in the Fig. 3a and b with different contrasts.

The newly constructed solid-phase diagram of the GeTe- Bi_2Te_3 -Te system matches the results of the EMF measurements of the

Table 2

Temperature dependences of the EMF for the cell of type (1) for alloys of the Ge-Bi-Te system in the temperature range of 300–450 K. Values of the coefficients a and b obtained through linear least squares analysis of the measured E vs. T values with the cell (1) at protective argon atmosphere $p = 0.6 \cdot 10^5$ Pa; n is the number of experimental points used in the calculations ($n \geq 20$); k – Student's coefficient at 0.95 level of confidence*.

Phase region	$E, \text{ mV} = a + bT + \bar{t}u_E(T)$
$\text{GeBi}_2\text{Te}_4 + \text{Ge}_2\text{Bi}_2\text{Te}_5 + \text{Te}$	$57.81 + 0.0385T \pm 2 \left[\frac{1.2}{30} + 2.0 \cdot 10^{-5} (T - 376.7)^2 \right]^{1/2}$
$\text{Ge}_2\text{Bi}_2\text{Te}_5 + \text{Ge}_3\text{Bi}_2\text{Te}_6 + \text{Te}$	$35.81 + 0.0430T \pm 2 \left[\frac{1.5}{30} + 2.5 \cdot 10^{-5} (T - 376.7)^2 \right]^{1/2}$
$\text{Ge}_3\text{Bi}_2\text{Te}_6 + \text{Ge}_4\text{Bi}_2\text{Te}_7 + \text{Te}$	$20.78 + 0.0478T \pm 2 \left[\frac{2.1}{30} + 2.1 \cdot 10^{-5} (T - 377.4)^2 \right]^{1/2}$

* Standard uncertainties u are $u_E = 0.8$ mV, $u_a = 0.4$, $u_b = 0.0039$, $u_T = 0.85$ K, $u_p = 10$ kPa.

concentration cells of type (1) at 400 K quite well. Fig. 4 displays the EMF isopleths at 400 K. EMF values of > 50 mol% Bi_2Te_3 composition region were taken from our previously published work in [29]. It can be seen that EMF measurements have three different values in 20–50 mol% Bi_2Te_3 phase region. These values confirm the existence of three different ternary compounds GeTe rich region as reported in [28] since values change sharply in the stoichiometric compositions of compounds. The emf measurements of these alloys were reproducible during the process and these findings allow for the calculation of the standard thermodynamic properties of the ternary intermediate compounds $\text{Ge}_2\text{Bi}_2\text{Te}_5$, $\text{Ge}_3\text{Bi}_2\text{Te}_6$, and $\text{Ge}_4\text{Bi}_2\text{Te}_7$.

Temperature dependences of EMF of type (1) cells for different alloys of the GeTe- Bi_2Te_3 -Te system are given in Fig. 5. It is seen that the EMF temperature dependence increases linearly with temperature in the 300–450 K range. Considering a linear connection between the EMF and temperature, the experimental data were analyzed using the least squares approach via OriginPro software. Experimentally obtained data for temperature (T_i), EMF (E_i) and data associated with the calculation steps for different alloys of the studied system are listed in Supplementary data – Table S1–3. Only specified crystalline phases were used for measurements.

To process the data from the EMF measurements, the procedure given in [37–39] is followed. The resulting linear equations of type (2) are reported in Table 2 in the following format, which is advised by the literature:

$$E = a + bT \pm t \left[(u_E^2/n) + u_b^2 \cdot (T - \bar{T})^2 \right]^{1/2} \quad (2)$$

In these equations, n is the number of pairs of E and T values; u_E and u_b – are dispersions of individual measurements of EMF and constant b ; \bar{T} – the average absolute temperature; t – the Student's t -test. At the confidence level of 95 % and $n \geq 20$, the Student's t -test ≤ 2 [37–39]. Using the obtained equations of type (2) and the following thermodynamic expressions:

$$\Delta \bar{G}_{\text{GeTe}} = -zFE \quad (3)$$

$$\Delta \bar{H}_{\text{GeTe}} = -z \left[E - T \left(\frac{\partial E}{\partial T} \right)_p \right] = -zFa \quad (4)$$

$$\Delta \bar{S}_{\text{GeTe}} = zF \left(\frac{\partial E}{\partial T} \right)_p = zFb \quad (5)$$

the relative partial molar functions of GeTe in the alloys of the studied

Table 3

Relative partial Gibbs energy ($-\Delta \bar{G}_{\text{GeTe}}$), enthalpy ($-\Delta \bar{H}_{\text{GeTe}}$), and entropy ($\Delta \bar{S}_{\text{GeTe}}$) of GeTe in the alloys of the GeTe- Bi_2Te_3 -Te system (298 K, $p = 0.1$ MPa). The presented confidence intervals in this table are calculated for the expanded uncertainty with 0.95 level of confidence.

Phase region	$-\Delta \bar{G}_{\text{GeTe}}$ kJ·mol ⁻¹	$-\Delta \bar{H}_{\text{GeTe}}$ kJ·mol ⁻¹	$\Delta \bar{S}_{\text{GeTe}}$, J/(K mol)
$\text{Ge}_2\text{Bi}_2\text{Te}_5 + \text{GeBi}_2\text{Te}_4 + \text{Te}$	13.37 ± 0.08	13.37 ± 0.08	7.41 ± 0.86
$\text{Ge}_3\text{Bi}_2\text{Te}_6 + \text{Ge}_2\text{Bi}_2\text{Te}_5 + \text{Te}$	9.39 ± 0.09	6.91 ± 0.37	8.32 ± 0.97
$\text{Ge}_4\text{Bi}_2\text{Te}_7 + \text{Ge}_3\text{Bi}_2\text{Te}_6 + \text{Te}$	6.76 ± 0.08	4.01 ± 0.34	9.22 ± 0.89

Table 4

Relative partial Gibbs energy ($-\Delta \bar{G}_{\text{Ge}}$), enthalpy ($-\Delta \bar{H}_{\text{Ge}}$), and entropy ($\Delta \bar{S}_{\text{Ge}}$) of germanium in the alloys of the GeTe- Bi_2Te_3 -Te system (298 K, $p = 0.1$ MPa). The presented confidence intervals in this table are calculated for the expanded uncertainty with 0.95 level of confidence.

Phase region	$-\Delta \bar{G}_{\text{Ge}}$ kJ·mol ⁻¹	$-\Delta \bar{H}_{\text{Ge}}$ kJ·mol ⁻¹	$\Delta \bar{S}_{\text{Ge}}$, J/(K mol)
$\text{Ge}_2\text{Bi}_2\text{Te}_5 + \text{GeBi}_2\text{Te}_4 + \text{Te}$	66.24 ± 0.17	60.66 ± 0.73	18.7 ± 1.93
$\text{Ge}_3\text{Bi}_2\text{Te}_6 + \text{Ge}_2\text{Bi}_2\text{Te}_5 + \text{Te}$	62.26 ± 0.18	56.41 ± 0.77	19.6 ± 1.97
$\text{Ge}_4\text{Bi}_2\text{Te}_7 + \text{Ge}_3\text{Bi}_2\text{Te}_6 + \text{Te}$	59.63 ± 0.17	53.51 ± 0.74	20.5 ± 1.94

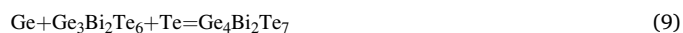
system at 450 K were calculated. Obtained results are given in Table 3.

Then, using information from Table 2 and the following equation, relative partial molar functions of germanium in the GeTe- Bi_2Te_3 -Te composition area were calculated using expressions (6). It should be noted that the difference between the partial molar functions of germanium for the left and right electrodes of the cell type (1) corresponds to the relative partial molar functions of GeTe in alloys.

$$\Delta \bar{Z}_{\text{Ge}}(\text{Ge-Bi-Te}) = \Delta \bar{Z}_{\text{Ge}}(\text{GeTe}) + \Delta \bar{Z}_{\text{GeTe}}(\text{Ge-Bi-Te}) \quad (6)$$

The thermodynamic values of germanium were taken from [40] in our calculations. Obtained results are listed in Table 4.

Considering the stability of coexisting phase compositions in the studied phase regions, the standard integral thermodynamic functions of the ternary compounds – $\text{Ge}_2\text{Bi}_2\text{Te}_5$, $\text{Ge}_3\text{Bi}_2\text{Te}_6$, and $\text{Ge}_4\text{Bi}_2\text{Te}_7$ were calculated using the virtual-cell reactions [37–39]. According to the solid-phase equilibria diagram shown in Fig. 1, the values of the relative partial molar functions of germanium in the different phase regions are thermodynamic functions of the following virtual-cell reaction expressions (7)–(9) (all substances in their stable crystallographic forms):



In accordance with these reactions, the integral thermodynamic functions of the ternary compounds were calculated by equations below (10)–(15):

$$\Delta_f Z^\circ(\text{Ge}_2\text{Bi}_2\text{Te}_5) = \Delta \bar{Z}_{\text{Ge}} + \Delta_f Z^\circ(\text{GeBi}_2\text{Te}_4) \quad (10)$$

$$\Delta_f Z^\circ(\text{Ge}_3\text{Bi}_2\text{Te}_6) = \Delta \bar{Z}_{\text{Ge}} + \Delta_f Z^\circ(\text{Ge}_2\text{Bi}_2\text{Te}_5) \quad (11)$$

$$\Delta_f Z^\circ(\text{Ge}_4\text{Bi}_2\text{Te}_7) = \Delta \bar{Z}_{\text{Ge}} + \Delta_f Z^\circ(\text{Ge}_3\text{Bi}_2\text{Te}_6) \quad (12)$$

$$S^\circ(\text{Ge}_2\text{Bi}_2\text{Te}_5) = \Delta \bar{S}_{\text{Ge}} + S^\circ(\text{Ge}) + S^\circ(\text{Te}) + S^\circ(\text{GeBi}_2\text{Te}_4) \quad (13)$$

$$S^\circ(\text{Ge}_3\text{Bi}_2\text{Te}_6) = \Delta \bar{S}_{\text{Ge}} + S^\circ(\text{Ge}) + S^\circ(\text{Te}) + S^\circ(\text{Ge}_2\text{Bi}_2\text{Te}_5) \quad (14)$$

$$S^\circ(\text{Ge}_4\text{Bi}_2\text{Te}_7) = \Delta \bar{S}_{\text{Ge}} + S^\circ(\text{Ge}) + S^\circ(\text{Te}) + S^\circ(\text{Ge}_3\text{Bi}_2\text{Te}_6) \quad (15)$$

The standard entropies of Ge (31.13 ± 0.30 J·K⁻¹·mol⁻¹), and Te (49.50 ± 0.21 J·K⁻¹·mol⁻¹) [41] and also thermodynamic data for

Table 5

Standard integral Gibbs energy ($\Delta_f G^\circ$), enthalpy ($\Delta_f H^\circ$) of formation, and entropy (S°) of binary and ternary phases of the Ge-Bi-Te system at temperature $T = 298$ K and pressure $p = 0.1$ MPa. The standard deviations were calculated by the error accumulation method using data of Table 4 and Refs. [41,42].

Phase	$-\Delta_f G^\circ$ (298 K)	$-\Delta_f H^\circ$ (298 K)	S° (298 K)	Ref.
	$\text{kJ}\cdot\text{mol}^{-1}$		$\text{J}/(\text{K}\cdot\text{mol})$	
$\beta(\text{Ge}_{0.05}\text{Bi}_{1.9}\text{Te}_{2.9})$	77.5 ± 0.2	79.2 ± 0.6	246.8 ± 3.0	[29]
$\beta(\text{Ge}_{0.1}\text{Bi}_{1.8}\text{Te}_{2.8})$	77.9 ± 0.2	79.0 ± 0.6	239.3 ± 3.0	[29]
$\text{GeBi}_6\text{Te}_{10}$	313.4 ± 0.8	312.8 ± 2.5	865.6 ± 11.7	[29]
GeBi_4Te_7	234.2 ± 0.6	231.7 ± 1.9	611.0 ± 8.7	[29]
GeBi_2Te_4	153.6 ± 0.4	149.8 ± 1.3	354.2 ± 5.6	[29]
$\text{Ge}_2\text{Bi}_2\text{Te}_5$	219.8 ± 0.6	210 ± 2.0	453.5 ± 8.1	This work
$\text{Ge}_2\text{Bi}_2\text{Te}_5(\text{Ag})^*$	286.5 ± 18.2	366.2 ± 21.6	155.6 ± 4.8	[30]
$\text{Ge}_3\text{Bi}_2\text{Te}_6$	282.1 ± 0.8	266.9 ± 2.8	553.7 ± 10.6	This work
$\text{Ge}_3\text{Bi}_2\text{Te}_6(\text{Ag})^*$	379.8 ± 32.5	495.6 ± 34.5	115.0 ± 6.9	[30]
$\text{Ge}_4\text{Bi}_2\text{Te}_7$	341.7 ± 1.0	320.4 ± 3.6	654.8 ± 13.1	This work
$\text{Ge}_4\text{Bi}_2\text{Te}_7(\text{Ag})^*$	461.0 ± 39.2	608.2 ± 48.4	90.5 ± 8.1	[30]

* – phases saturated by silver.

Bi_2Te_3 [42] were used in our calculations along with our experimental data (Table 4). These data are in good agreement with the data recommended in well-known reference books [43–45]. Obtained integral thermodynamic quantities are tabulated in Table 5 together with our reported values in [29] and values obtained by authors of [30]. In all calculations, the estimated standard deviations were determined by the accumulation of errors.

A comparison of our results with the data of [30] shows their significant discrepancy. At the same time, the numerical values of $\Delta_f G^\circ$ and $\Delta_f H^\circ$ presented by the authors of [30] are higher, and the standard entropies are much lower than our data. It should be noted that the values of the standard entropies according to the data of [30] are several times lower than the sum of the entropies of constituent elements or binary compounds, which is extremely unlikely. The studied compounds have complex crystal structures, which are characterized by high entropy values. On the other hand, the authors of [30] studied standard thermodynamic parameters of the ternary compounds using phase equilibria information of different concentration area – a four-element space exhibits the properties of phases of variable composition. We assume that it is the main reason why the obtained values in this work deviate to some extent from the values published by [30] since the phase relationship is quite different in this concentration area.

4. Conclusion

Here, the results of a complex study of a phase relationship in the $\text{GeTe-Bi}_2\text{Te}_3\text{-Te}$ system at 400 K and thermodynamic parameters of GeTe-rich germanium-bismuth tellurides by powder XRD, SEM, and EMF method using liquid (the glycerol solution of KCl) electrolyte in 300–450 K temperature range were reported. The partial molar functions of GeTe in the alloys of the $\text{GeTe-Bi}_2\text{Te}_3\text{-Te}$ system were reproduced by the calculations using obtained EMF data. These values and the partial molar functions of germanium in GeTe were used to determine the corresponding partial functions of germanium in the alloys. Standard thermodynamic functions of formation and standard entropies of ternary compounds, namely $\text{Ge}_2\text{Bi}_2\text{Te}_5$, $\text{Ge}_3\text{Bi}_2\text{Te}_6$, and $\text{Ge}_4\text{Bi}_2\text{Te}_7$ were calculated using determined virtual-cell reactions according to the solid-phase equilibrium diagram.

CRedit authorship contribution statement

E.N. Orujlu: Writing – original draft, Software, Methodology,

Investigation, Formal analysis. D.M. Babanly: Writing – review & editing, Supervision, Project administration, Methodology, Investigation, Conceptualization. T.M. Alakbarova: Resources, Investigation, Formal analysis. N.I. Orujov: Investigation, Formal analysis, Data curation. M.B. Babanly: Writing – review & editing, Supervision, Project administration, Methodology, Investigation, Conceptualization.

Declaration of competing interest

The authors declare that they have no known competing financial interests or personal relationships that could have appeared to influence the work reported in this paper.

Data availability

No data was used for the research described in the article.

Acknowledgment

The work was supported by the Azerbaijan Science Foundation - Grant N^o AEF-MCG-2022-1(42)-12/10/4-M-10.

Appendix A. Supplementary data

Supplementary data to this article can be found online at <https://doi.org/10.1016/j.jct.2024.107323>.

References

- [1] S. Roychowdhury, M. Samanta, S. Perumal, K. Biswas, Germanium chalcogenide thermoelectrics: electronic structure modulation and low lattice thermal conductivity, *Chem. Mater.* 30 (17) (2018) 5799–5813, <https://doi.org/10.1021/acs.chemmater.8b02676>.
- [2] M. Rakshit, D. Jana, D. Banerjee, General strategies to improve thermoelectric performance with an emphasis on tin and germanium chalcogenides as thermoelectric materials, *J. Mater. Chem. A* 10 (2022) 6872–6926, <https://doi.org/10.1039/D1TA10421G>.
- [3] P. Hosseini, C. Wright, H. Bhaskaran, An optoelectronic framework enabled by low-dimensional phase-change films, *Nature* 511 (2014) 206–211, <https://doi.org/10.1038/nature1348>.
- [4] C. Ríos, P. Hosseini, R.A. Taylor, H. Bhaskaran, Color depth modulation and resolution in phase-change material nanodisplays, *Adv. Mater.* 28 (23) (2016) 4720–4726, <https://doi.org/10.1002/adma.201506238>.
- [5] C. Ríos, M. Stegmaier, P. Hosseini, D. Wang, T. Scherer, C.D. Wright, H. Bhaskaran, W.H.P. Pernice, Integrated all-photon non-volatile multi-level memory, *Nat. Photon.* 9 (2015) 725–732, <https://doi.org/10.1038/nphoton.2015.182>.
- [6] Z. Cheng, C. Ríos, N. Youngblood, C.D. Wright, W.H.P. Pernice, H. Bhaskaran, Device-level photonic memories and logic applications using phase-change materials, *Adv. Mater.* 30 (2018) 1802435, <https://doi.org/10.1002/adma.201802435>.
- [7] W. Zhang, R. Mazzarello, M. Wuttig, E. Ma, Designing crystallization in phase-change materials for universal memory and neuro-inspired computing, *Nat. Rev. Mater.* 4 (2019) 150–168, <https://doi.org/10.1038/s41578-018-0076-x>.
- [8] J. Zhu, T. Zhang, Y. Yang, R. Huang, A comprehensive review on emerging artificial neuromorphic devices, *Appl. Phys. Rev.* 7 (2020) 011312, <https://doi.org/10.1063/1.5118217>.
- [9] M. Xu, X. Mai, J. Lin, W. Zhang, Y. Li, Y. He, H. Tong, X. Hou, P. Zhou, X. Miao, Recent advances on neuromorphic devices based on chalcogenide phase-change materials, *Adv. Funct. Mater.* 30 (2020) 2003419, <https://doi.org/10.1002/adfm.202003419>.
- [10] T. Matsunaga, N. Yamada, Structural investigation of GeSb_2Te_4 : a high-speed phase-change material, *Phys. Rev. B* 69 (2004) 104111, <https://doi.org/10.1103/PhysRevB.69.104111>.
- [11] B.S. Lee, J.R. Abelson, Investigation of the optical and electronic properties of $\text{Ge}_2\text{Sb}_2\text{Te}_5$ phase change material in its amorphous, cubic, and hexagonal phases, *J. Appl. Phys.* 97 (2005) 093509, <https://doi.org/10.1063/1.1884248>.
- [12] J.-J. Wang, Y.-Z. Xu, R. Mazzarello, M. Wuttig, W. Zhang, A review on disorder-driven metal-insulator transition in crystalline vacancy-rich GeSbTe phase-change materials, *Materials* 10 (2017) 862, <https://doi.org/10.3390/ma10080862>.
- [13] J. Tominaga, The design and application on interfacial phase-change memory, *Phys. Status Solidi RRL* 13 (2019) 180053, <https://doi.org/10.1002/pssr.201800539>.
- [14] P. Guo, A.M. Sarangan, I. Agha, A review of germanium-antimony-telluride phase change materials for non-volatile memories and optical modulators, *Appl. Sci.* 9 (2019) 530, <https://doi.org/10.3390/app9030530>.

- [15] Z. Song, R. Wang, Y. Xue, S. Song, The “gene” of reversible phase transformation of phase change materials: octahedral motif, *Nano Res.* 15 (2022) 765–772, <https://doi.org/10.1007/s12274-021-3570-1>.
- [16] J. Kim, J. Kim, S.-H. Jhi, Prediction of topological insulating behavior in crystalline Ge-Sb-Te, *Phys. Rev. B* 82 (2010) 201312(R), <https://doi.org/10.1103/PhysRevB.82.201312>.
- [17] J. Kim, S.-H. Jhi, Emerging topological insulating phase in Ge-Sb-Te compounds, *Phys. Status Solidi B* 249 (2012) 1874–1879, <https://doi.org/10.1002/pssb.201200369>.
- [18] I.V. Silkin, Y.M. Koroteev, G. Bihlmayer, E.V. Chulkov, Influence of the Ge-Sb sublattice atomic composition on the topological electronic properties of $\text{Ge}_2\text{Sb}_2\text{Te}_5$, *Appl. Surf. Sci.* 267 (2013) 169–172, <https://doi.org/10.1016/j.apsusc.2012.09.017>.
- [19] K. Okamoto, K. Kuroda, H. Miyahara, K. Miyamoto, T. Okuda, Z.S. Aliev, M. B. Babanly, I.R. Amiraslanov, K. Shimada, K. Namatame, M. Taniguchi, D. A. Samorokov, T.V. Menshchikova, E.V. Chulkov, A. Kimura, Observation of a highly spin-polarized topological surface state in GeBi_2Te_4 , *Phys. Rev. B* 86 (19) (2012) 195304, <https://doi.org/10.1103/PhysRevB.86.195304>.
- [20] M. Nurmamat, K. Okamoto, S. Zhu, T.V. Menshchikova, I.P. Rusinov, V. O. Korostelev, K. Miyamoto, T. Okuda, T. Miyashita, X. Wang, Y. Ishida, K. Sumida, E.F. Schwier, M. Ye, Z.S. Aliev, M.B. Babanly, I.R. Amiraslanov, E.V. Chulkov, K. A. Kokh, O.E. Tereshchenko, K. Shimada, S. Shin, A. Kimura, Topologically non-trivial phase-change compound GeSb_2Te_4 , *ACS Nano* 14 (7) (2020) 9059–9065, <https://doi.org/10.1021/acsnano.0c04145>.
- [21] A. Sterzi, G. Manzoni, A. Crepaldi, F. Cilento, M. Zacchigna, M. Leclerc, P. Bugnon, A. Magrez, H. Berger, L. Petaccia, F. Parmigiani, Probing band parity inversion in the topological insulator GeBi_2Te_4 by linear dichroism in ARPES, *J. Electron. Spectrosc. Relat. Phenom.* 225 (2018) 23–27, <https://doi.org/10.1016/j.elspec.2018.03.004>.
- [22] M.B. Babanly, E.V. Chulkov, Z.S. Aliev, A.V. Shevelkov, I.R. Amiraslanov, Phase Diagrams in materials science of topological insulators based on metal chalcogenides, *Russ. J. Inorg. Chem.* 62 (2017) 1703–1729, <https://doi.org/10.1134/S0036023617130034>.
- [23] N.X. Abrikosov, G.T. Danilova-Dobryakova, Study of the $\text{GeTe-Bi}_2\text{Te}_3$ phase diagram, *Izv. Akad. Nauk SSSR, Neorg. Mater.* 1 (1965) 57–61, in Russian.
- [24] L.E. Shelimova, O.G. Karpinskii, V.S. Zemskov, P.P. Konstantinov, Structural and electrical properties of layered tetradymite-like compounds in the $\text{GeTe-Bi}_2\text{Te}_3$ and $\text{GeTe-Sb}_2\text{Te}_3$ systems, *Inorg. Mater.* 36 (3) (2000) 235, <https://doi.org/10.1007/BF02757928>.
- [25] L.E. Shelimova, O.G. Karpinskii, V.I. Kosyakov, V.A. Shestakov, V.S. Zemskov, F. A. Kuznetsov, Homologous series of layered tetradymite-like compounds in Bi-Te and $\text{GeTe-Bi}_2\text{Te}_3$ systems, *J. Struct. Chem.* 41 (1) (2000) 81–87, <https://doi.org/10.1007/BF02684732>.
- [26] O.G. Karpinskii, L.E. Shelimova, M.A. Kretova, V.S. Zemskov, X-ray diffraction study of Ge-Bi-Te mixed-layer ternary compounds, *Inorg. Mater.* 36 (2000) 1108–1113, <https://doi.org/10.1007/BF02758926>.
- [27] L.E. Shelimova, O.G. Karpinskii, P.P. Konstantinov, E.S. Avilov, M.A. Kretova, V. S. Zemskov, Crystal structures and thermoelectric properties of layered compounds in the ATe-Bi₂Te₃ (A = Ge, Sn, Pb) systems, *Inorg. Mater.* 40 (5) (2004) 451–460, <https://doi.org/10.1023/B:INMA.0000027590.43038.a8>.
- [28] T.M. Alakbarova, H.-J. Meyer, E.N. Orujlu, I.R. Amiraslanov, M.B. Babanly, Phase equilibria of the $\text{GeTe-Bi}_2\text{Te}_3$ quasi-binary system in the range 0–50 mol% Bi_2Te_3 , *Ph. Transit.* 94 (5) (2021) 366–375, <https://doi.org/10.1080/01411594.2021.1937625>.
- [29] T. Alakbarova, E. Orujlu, D. Babanly, S. Imamaliyeva, M. Babanly, Solid-phase equilibria in the $\text{GeBi}_2\text{Te}_4\text{-Bi}_2\text{Te}_3\text{-Te}$ system and thermodynamic properties of compounds of the $\text{GeTe-mBi}_2\text{Te}_3$ homologous series, *Phys. Chem. Solid St.* 23 (1) (2022) 25–33, <https://doi.org/10.15330/pcss.23.1.25-33>.
- [30] M. Moroz, F. Tesfaye, P. Demchenko, M. Prokhorenko, O. Pereviznyk, B. Rudyk, L. Soliak, D. Lindberg, O. Reshetnyak, L. Hupa, in: *Phase Equilibria in the Ag-ge-bi-te System and Thermodynamic Properties of the nGeTe-mBi₂Te₃ (n, m = 1–4) Layered Compounds*, Springer, Cham, 2022, pp. 60–73, https://doi.org/10.1007/978-3-030-92381-5_7.
- [31] M. Moroz, F. Tesfaye, P. Demchenko, E. Mastronardo, O. Mysina, M. Prokhorenko, S. Prokhorenko, D. Lindberg, O. Reshetnyak, L. Hupa, Experimental thermodynamic characterization of the chalcopyrite-based compounds in the Ag-In-Te system for a potential thermoelectric application, *Energies* 15 (2022) 8180, <https://doi.org/10.3390/en15218180>.
- [32] M. Moroz, F. Tesfaye, P. Demchenko, M. Prokhorenko, S. Prokhorenko, D. Lindberg, O. Reshetnyak, L. Hupa, Synthesis and Thermodynamic Investigation of Energy Materials in the Ag-Te-Cl System by the Solid-State Galvanic Cells, *JOM.* 73 (2021) 1487–1494, <https://doi.org/10.1007/s11837-021-04619-9>.
- [33] M.V. Voronin, E.G. Osadchii, Determination of thermodynamic properties of triple phases formed in different regions of phase diagram of the Ag-Bi-S system using EMF measurements, *Russ. J. Electrochem.* 499 (2013) 741–746, <https://doi.org/10.1134/S1023193513080211>.
- [34] E.G. Osadchii, V.B. Polyakov, V.O. Osadchii, Synthesis, X-ray data, and thermodynamic properties of the AgTe_3 high-pressure phase in the Ag-Te system, *J. Alloys Compd.* 855 (1) (2021) 157407, <https://doi.org/10.1016/j.jallcom.2020.157407>.
- [35] E.N. Orujlu, Z.S. Aliev, Y.I. Jafarov, E.I. Ahmadov, M.B. Babanly, Thermodynamic study of manganese tellurides by the electromotive force method, *Condens. Matter. Phys.* 23 (2) (2021) 273, <https://doi.org/10.17308/kcmf.2021.23/3438>.
- [36] S.Z. Imamaliyeva, D.M. Babanly, V.A. Qasymov, M.B. Babanly, Solid-phase Relationships in the $\text{Tl}_2\text{Te-Tl}_2\text{Te}_3\text{-TlTlTe}_2$ System and Thermodynamic Properties of Thallium-Terbium Tellurides, *JOM.* 73 (2021) 1503–1510, <https://doi.org/10.1007/s11837-021-04623-z>.
- [37] M.B. Babanly, Y.A. Yusibov, N.B. Babanly, Electromotive Force and Measurement in Several Systems, in: S. Kara (ed.), *IntechOpen*, London, 2011, pp. 57–78. <https://doi.org/10.5772/28934>.
- [38] A.G. Morachevsky, G.F. Voronin, V.A. Geyderich, I.B. Kutsenok, *Electrochemical research methods in the thermodynamics of metallic systems*, Akademkniga Publ, Moscow, 2003 in Russian.
- [39] M.B. Babanly, Y.A. Yusibov, *Electrochemical methods in thermodynamics of inorganic systems*, BSU Publ, Baku, 2011 in Russian.
- [40] T.M. Alakbarova, Thermodynamic properties of germanium telluride, *New Mater. Compd. Appl.* 5 (1) (2021) 59–65.
- [41] Database of thermal constants of substances. Digital version. Eds.: V.S. Iorish and V.S. Yungman. 2006. <http://www.chem.msu.ru/cgi-bin/tkv.pl>.
- [42] G.S. Hasanova, A.I. Aghazade, S.Z. Imamaliyeva, Y.A. Yusibov, M.B. Babanly, Refinement of the phase diagram of the Bi-Te system and the thermodynamic properties of lower bismuth tellurides, *JOM.* 73 (5) (2021) 1511–1521, <https://doi.org/10.1007/s11837-021-04621-1>.
- [43] O. Kubaschewski, C.B. Alcock, P.J. Spenser, *Materials Thermochemistry*, Pergamon Press, Oxford, 1993.
- [44] I. Barin, *Thermochemical Data of Pure Substances*, 3rd Ed., Wiley-VCH, Weinheim, 2008.
- [45] K.C. Mills, *Thermodynamic data for inorganic sulphides, selenides, and tellurides*, Butterworth, London, 1974.